MADRID
inter.noise 2019
June 16 - 19
NOISE CONTROL FOR A BETTER ENVIRONMENT

Distortion of anisotropic turbulence spectrum in the vicinity of aerofoil leading edge

Shen, Zhen[1]
The Hong Kong University of Science and Technology
Clear Water Bay, Kowloon, Hong Kong SAR, China

Zhang, Xin[2]
HKUST Shenzhen Research Institute
Shenzhen 518057, China

ABSTRACT

This work numerically investigates the distortion of turbulence spectrum in the vicinity of aerofoil leading edge, which has a significant impact on the turbulence-aerofoil interaction noise. By applying different degrees of anisotropy in the incident turbulence spectrum, the effects of aerofoil thickness and angle of attack on distorted turbulence spectrum and interaction noise are investigated in the computational aeroacoustics simulations. It is shown that the turbulent eddies stretched in the streamwise direction have the slightest distortion of turbulence spectrum for symmetric aerofoils at zero incidence, compared with the isotropic case and the transversely stretched case. In addition, the increase of angle of attack has a significant impact on the anisotropic turbulence-aerofoil interaction noise, leading to the noise increase in the axially stretched case and noise reduction in the transversely stretched case. Finally, a modified far field noise prediction model is proposed by using the distorted turbulence spectrum in the vicinity of aerofoil leading edge, in order to account for the effect of real aerofoil geometries.

Keywords: Computational aeroacoustics, Synthetic turbulence, Turbulence-aerofoil interaction noise
I-INCE Classification of Subject Number: 10

1. INTRODUCTION

Turbulence-aerofoil interaction noise is regarded as a significant contributor to the broadband noise in turbofan engines, which is owing to the interactions of incoming

[1]zshenaf@connect.ust.hk
[2]aexzhang@ust.hk

turbulent flow with the fan blades and Outlet Guide Vanes (OGVs). The turbulence-aerofoil interaction noise model for a flat plate was proposed by Amiet [1] who assumed that turbulent gusts were convected by a uniform mean flow. However, compared with a flat plate, the turbulence-aerofoil interaction noise is reduced at high frequencies for a thick aerofoil, which is partly due to the distortion of the mean flow in the vicinity of the leading edge [2]. Therefore, the effects of real aerofoil geometries on turbulence-aerofoil interaction noise cannot be ignored at high wavenumbers.

1.1.1. Previous work

Previous studies have analysed the main factors that affect turbulence-aerofoil interaction noise, such as the angle of attack (AoA), camber and aerofoil thickness. Many of the previous methodologies are based on the pioneering work by Sears [3] and Amiet [1].

In order to obtain the correct prediction of leading edge noise, the unsteady lift response must be calculated accurately as a significant step. The incompressible analytical model has been initially addressed by Sears [3], where the unsteady lift and moment from an aerofoil encountering periodic perturbation was predicted, by solving the Laplace equation representing the incompressible potential flow. This analytical model was extended to consider compressibility effects by Amiet [1], who put forward an analytical expression for the leading edge noise emissions produced by a flat plate encountering oncoming turbulent stream, which agrees well with the experimental results when $\Lambda \equiv MK_xd > 1$, where M is the free stream Mach number, K_x is the particular value for chordwise wavenumber, d is the semi span of the aerofoil. For small values of Λ which is smaller than 1, the agreement between analytical solution and experiment data can be still reasonable only if Λ was made small due to the relatively small value of Mach number. Although the flat plate theory neglects the effects of real aerofoil geometry on noise generation, inspiration and enlightenment contained in this analytical model have laid a solid foundation for the further study. For example, Amiet [1] indicated that the transverse velocity disturbance bears principal responsibility for the noise generation of a flat plate at zero angle of attack, which was demonstrated in Gill *et al.*'s numerical simulations [4] using Fourier mode methods with one-component, two-component, and three-component synthesized turbulence. Gill *et al.* [4] also showed that the streamwise and spanwise fluctuating velocity components are negligible for symmetric aerofoils at zero incidence interacting with isotropic turbulence. Meanwhile, the impacts of camber and angle of attack on the interaction noise can be neglected for the isotropic case. However, Gill *et al.* [4] speculated that the interaction noise could be sensitive to the angle of attack for the anisotropic case.

Some attempts have been made to make the current theory applicable to real aerofoil geometry, for instance, on the basis of flat plate theory [1], Guidati and Wagner [5] developed a model for sound emission from the interaction between incoming vortical gusts and isolated aerofoil, where the vorticity is convected by the background potential flow which is incompressible and inviscid. In this regime, the relationship between the stagnation enthalpy and the source term containing vorticity and flow velocity can be transformed into Helmholtz equation, by using harmonic convention. Once the source term is known, the Helmholtz equation can be solved through the use of boundary-element method. Following Guidati and Wagner's work [5], Moriarty *et al.* [6] combined Amiet's model [1] predicting the absolute sound level of flat plate and Guidati and Wagner's frequency dependent correction [5] compared with actual aerofoil, then a

10 dB adjustment was made to promote the accuracy of predicted results. However, the major drawback of Moriarty *et al.*'s model [6] is that the 10 dB adjustment may not be applicable to the general case, which means that this correction factor is restricted to his own numerical examples.

On the basis of Green's function accounting for the aerofoil thickness, Gershfeld [7] predicted the sound from the diffraction of turbulence by the leading edge of a thick aerofoil, suggesting that the aerofoil thickness tends to exponentially decrease the leading edge noise. Moreau *et al.* [8] proposed camber and thickness corrections to the radiation integral. However, the thickness correction was smaller than the sound reduction in the experiments. Then, Moreau *et al.* [8] postulated the modified transverse velocity spectrum to account for the distortion of small eddies, which was based on the rapid distortion theory (RDT) around bluff bodies developed by Hunt [9]. Similar implementation of the rapid distortion theory was also proposed by Santana *et al.* [10] who put forward a modified von Kármán energy spectrum following a -10/3 power law at high frequencies, in order to account for the turbulence distortion in the vicinity of the leading edge. The modified von Kármán energy spectrum was then introduced in Amiet's theory, reproducing the spanwise-varying turbulence statistics through inverse strip method, which presented improved leading edge noise predictions if distorted turbulence statistics were sampled at appropriate position.

Glegg and Devenport [11] used a panel method to predict unsteady loading and noise radiation from flat plate and real aerofoils. However, this method was restricted to incompressible turbulent flow and the only response to spanwise incident vorticity. Based on this incompressible vortex panel method, Devenport *et al.* [12] studied the effect of angle of attack and camber for different aerofoil geometries, showing that the effects of angle of attack and camber were small if the inflow turbulence spectrum was isotropic, whereas a 10 dB increase in the sound pressure level was found at 12° angle of attack compared with the zero incidence case for a NACA 0015 aerofoil interacting with anisotropic turbulence stretched in the axial direction. This implies that the effects of aerofoil geometries and angle of attack will be significantly different if anisotropy is considered in the inflow turbulence spectrum.

1.1.2. Aims and objectives

In this work, a more general case considering the effect of anisotropy is studied, which is concentrated on the following objectives:

- To investigate the distortion of anisotropic turbulence spectrum by the non-uniform mean flow around the aerofoil leading edge. By applying different stretching ratios in the inflow turbulence spectrum, the effects of aerofoil geometries and angle of attack on distorted turbulence spectrum and far field interaction noise will be studied systematically.

- To propose a modified analytical model of the far field noise prediction based on Amiet's theory. The undistorted transverse velocity spectrum in the flat plate theory is replaced by the distorted turbulence statistics sampled at appropriate position.

The remaining part of this paper is organised as follows. Section 2 shows the distortion of one-dimensional spectra around a symmetric NACA 0012 aerofoil at zero incidence interacting with anisotropic turbulence. And the effect of angle of attack on turbulence distortion and interaction noise are presented in Section 3. Then, a modified analytical solution considering the influence of aerofoil thickness is proposed to improve the far field noise predictions, which is shown in Section 4. Section 5 gives the conclusions of this work.

2. DISTORTION OF ONE-DIMENSIONAL SPECTRA

In this section, the investigation of turbulence distortion is started with a symmetric NACA 0012 aerofoil at zero angle of attack. The chord length and semi-span length are set to be $c = 0.15\,\mathrm{m}$ and $d = 0.225\,\mathrm{m}$, respectively. The random-eddy-superposition (RES) technique developed previously by the author [13] is used in the numerical simulation to synthesize the income turbulence, which can realise varying degrees of anisotropy by applying various stretching ratios in the axisymmetric turbulence model from Kerschen and Gliebet [14]. As shown in figure 1(b), under Taylor's frozen turbulence assumption [15], the turbulent eddies introduced at the inlet section will be convected by the background mean flow, which can reproduce the major statistics of the three-dimensional axisymmetric turbulence. Then, the RES technique is combined with the linearised Euler equations (LEE) to predict the turbulence-aerofoil interaction noise in computational aeroacoustics simulations.

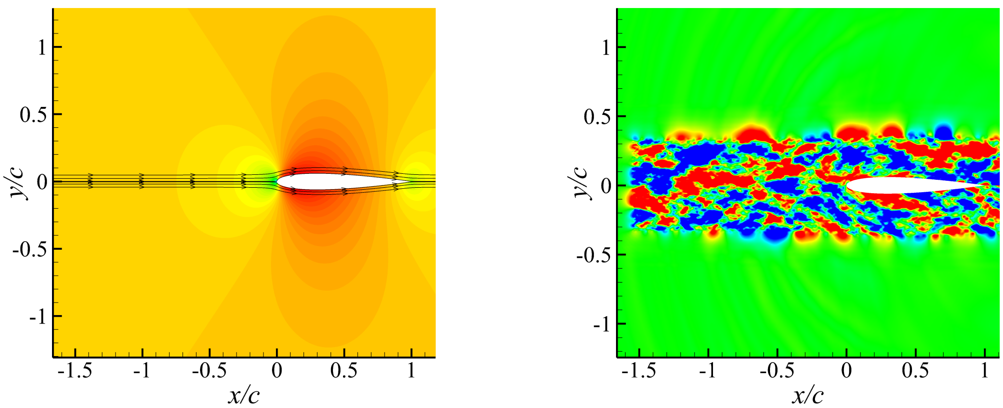

(a) Mean flow field around a NACA 0012 aerofoil at zero angle of attack.

(b) Non-dimensional fluctuating velocity in streamwise direction, u'/c_0.

Figure 1: Mean flow field and fluctuating velocity field around a NACA 0012 aerofoil at $M_\infty = 0.6$.

A line of monitoring points are placed along the stagnation line shown in figure 1(a), which start from a position away from the leading edge and end at the stagnation point. Figure 2 shows the distortion of one-dimensional energy spectra at different monitors immersed in the isotropic turbulence of Liepmann spectrum with $l_a = l_t = 0.008\,\mathrm{m}$, where l_a and l_t denote the axial and tangential length scales, respectively. As can be seen from figure 2, when the monitors get closer to the stagnation point, the one-dimensional energy spectra E_{11} decreases uniformly at all frequencies compared with the initial one-dimensional energy spectra without distortion, whereas E_{22} increases at low wavenumbers and decreases at high wavenumbers in the vicinity of the leading edge.

This phenomenon can be more clearly seen from the normalized one-dimensional spectra shown in figure 3, where the one-dimensional energy spectra are normalised

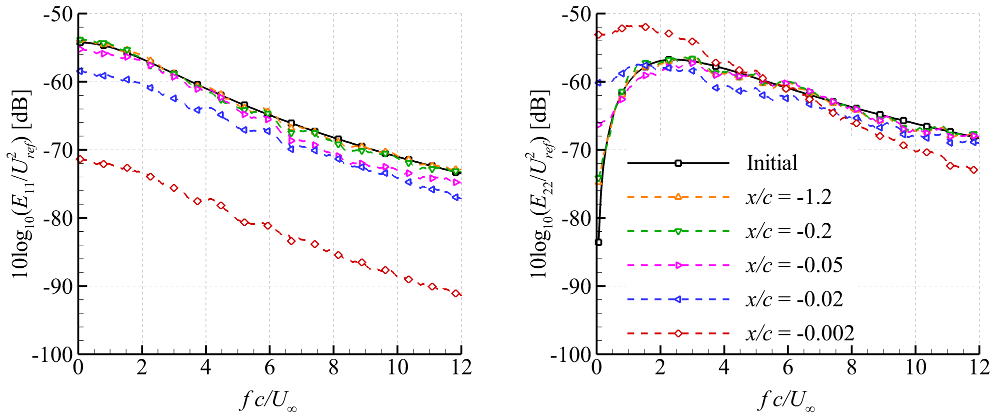

(a) E_{11}

(b) E_{22}

Figure 2: Distortion of one-dimensional energy spectra of isotropic turbulence impinging on a NACA 0012 aerofoil at $M_\infty = 0.6$.

by the undistorted spectra away from the leading edge. On the central streamline from $x/c = -1.2$ to $x/c = -0.2$, no evident difference can be detected compared with the initial spectra calculated by the theoretical expression. Distortion of turbulence energy spectra seems to be noticeable starting from $x/c = -0.05$. The one-dimensional energy spectra E_{11} start to decrease at reduced frequencies larger than 6. As the distance to the leading edge decreases, the downward trend tends to be evenly distributed throughout all the frequencies. As for the one-dimensional energy spectra E_{22}, the demarcation point at which the growing tendency ends and descending trend begins will move towards high-frequency range, with the decrease of the distance between the monitors and stagnation point.

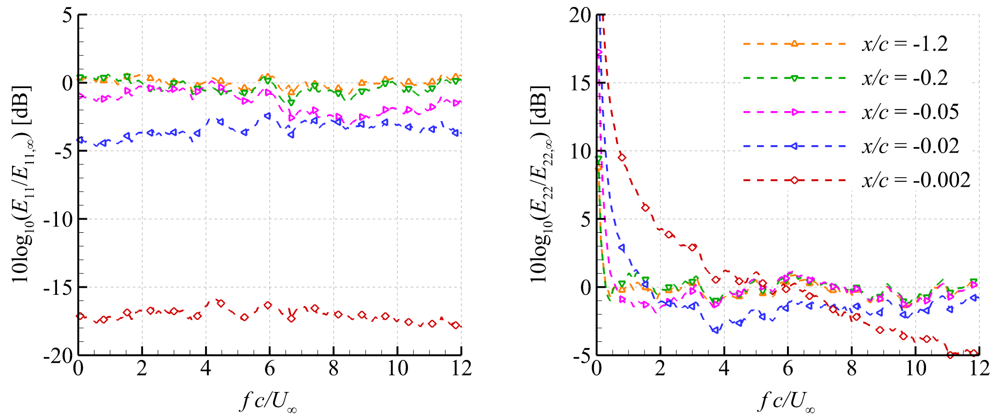

(a) Normalised E_{11}

(b) Normalised E_{22}

Figure 3: Distortion of normalized one-dimensional energy spectra of isotropic turbulence impinging on a NACA 0012 aerofoil at $M_\infty = 0.6$.

In order to account for the effect of anisotropy on the distortion of turbulence energy spectra, another two cases are considered. One is the anisotropic turbulence with axial stretching characterised by $l_a = 3/2\,l_t = 0.008\,\mathrm{m}$, the other one is the tangentially stretched turbulent flow with $l_a = 2/3\, l_t = 0.008\,\mathrm{m}$. The distortion of normalized streamwise energy spectra E_{11} considering the impact of anisotropy is shown in figure 4. Compared with the isotropic case shown in figure 3, distortion of streamwise energy spectra E_{11} for the transverse stretching case with $l_a = 2/3\, l_t = 0.008\,\mathrm{m}$ is the largest one, shaped like a concave function with the minimum distortion at the mid-frequency range. Whereas distortion seems to be smallest for the axial stretching case with $l_a = 3/2\, l_t = 0.008\,\mathrm{m}$, especially at high frequencies.

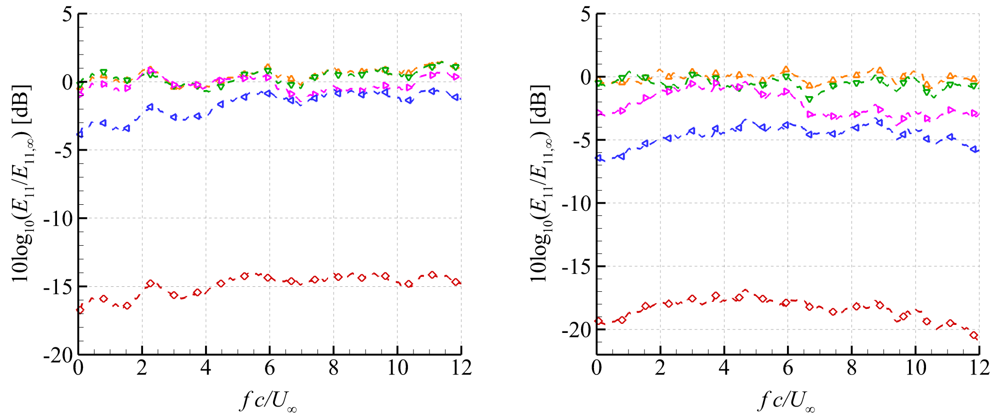

(a) $l_a = 3/2\, l_t = 0.008\,\mathrm{m}$ (b) $l_a = 2/3\, l_t = 0.008\,\mathrm{m}$

Figure 4: Distortion of normalized streamwise energy spectra E_{11} of anisotropic turbulence impinging on a NACA 0012 aerofoil at $M_\infty = 0.6$.

Similarly, as shown in figure 5, distortion of transverse energy spectra E_{22} for the axial stretching case is the smallest, which is embodied in the slightest reduction at high frequencies. On the contrary, the transverse stretching case shows the most significant decrease within the high-wavenumber range, which is even more remarkable than the isotropic case. This phenomenon is in accordance with our previous conclusion that the axial stretching will suppress the thickness-induced noise reduction [13]. It can be inferred that this inhibition mechanism stems from the minor distortion of the turbulence energy spectra at high frequencies by the mean flow when the turbulent flow is streamwisely stretched.

3. IMPACT OF AOA ON TURBULENCE DISTORTION AND INTERACTION NOISE

In this section, the effect of angle of attack on anisotropic turbulence distortion around thick aerofoil and the consequent interaction noise is investigated. A NACA 0012 aerofoil at $AoA = 4°$ is used in the numerical simulations, around which the mean flow is assumed to be inviscid with $M_\infty = 0.3$. These values of freestream Mach number and AoA will ensure a subsonic flow in the vicinity of the aerofoil leading edge and get rid of the instabilities in LEE simulations when dealing with highly sheared mean flow caused by large AoA.

Compared with the zero incidence cases, slight decreases at high frequencies can be seen in the distorted normalized streamwise energy spectra E_{11} for the $AoA = 4°$ cases, no matter what the anisotropy is. However, the relative changes in the distorted

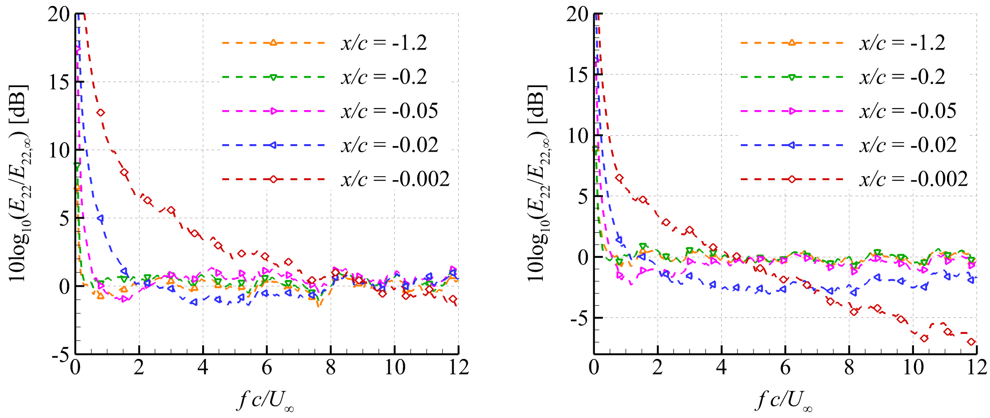

(a) $l_a = 3/2\, l_t = 0.008\,\mathrm{m}$ (b) $l_a = 2/3\, l_t = 0.008\,\mathrm{m}$

Figure 5: Distortion of normalized transverse energy spectra E_{22} of anisotropic turbulence impinging on a NACA 0012 aerofoil at $M_\infty = 0.6$.

normalized transverse energy spectra E_{22} seem to be quite different for cases with different stretching ratios. When the turbulent eddies are stretched in the transverse direction, E_{22} has witnessed a pronounced reduction especially at high frequencies. While E_{22} drops slightly at high frequencies for the isotropic case. The strangest change occurs in the anisotropic turbulence with axial stretching, where E_{22} increases at $x/c = -0.05$ and declines slightly at $x/c = -0.002$.

The relative changes in the distorted normalized transverse energy spectra E_{22} has further influenced the noise spectra shown in figure 6(a), where no apparent difference can be seen from the PWL spectra for a NACA 0012 aerofoil at $AoA = 0°$ and $4°$ interacting with isotropic turbulence. However, the increase of AoA seems to exert a strong influence on the leading edge noise from anisotropic turbulence. More specifically, an obvious increase in the PWL spectra can be found when the eddies are stretched in the streamwise direction, $l_a/l_t > 1$. On the contrary, for the anisotropic turbulence with transverse stretching, $l_t/l_a > 1$, the increase of incidence leads to the reduction in the PWL spectra especially at high frequencies, which can be clearly seen from the ΔPWL spectra defined as $\Delta\mathrm{PWL} = \mathrm{PWL}|_{AoA=4°} - \mathrm{PWL}|_{AoA=0°}$. The maximum ΔPWL is approximately 3.53 dB/Hz for the anisotropic turbulence with $l_a/l_t = 1.5$, presenting a relatively large disparity compared with the results from Gea-Aguilera *et al.* [16] who showed an increase of 1 dB at all frequencies. While the findings in this paper are consistent with Devenport *et al.* [12] who also suggested a strong influence of anisotropy on leading edge noise when $l_a/l_t = 2$.

Figure 7(a) shows the directivity pattern for a NACA 0012 aerofoil at different AoAs interacting with anisotropic turbulence. Compared with the zero incidence case where the incoming turbulence is isotropic, the directivity pattern of the $AoA = 4°$ case is rotated in the counter-clockwise direction, which is even more obvious than the cambered aerofoil cases. Such kind of counter-clockwise rotation effect will lead to the upstream noise increase and downstream noise decrease on the suction side of the aerofoil, while on the pressure side of the aerofoil, the OASPL at downstream observers is increased. This phenomenon also occurs in the anisotropic case with axial stretching, where the upstream noise increase is more remarkable on the suction side of the aerofoil. However, when the

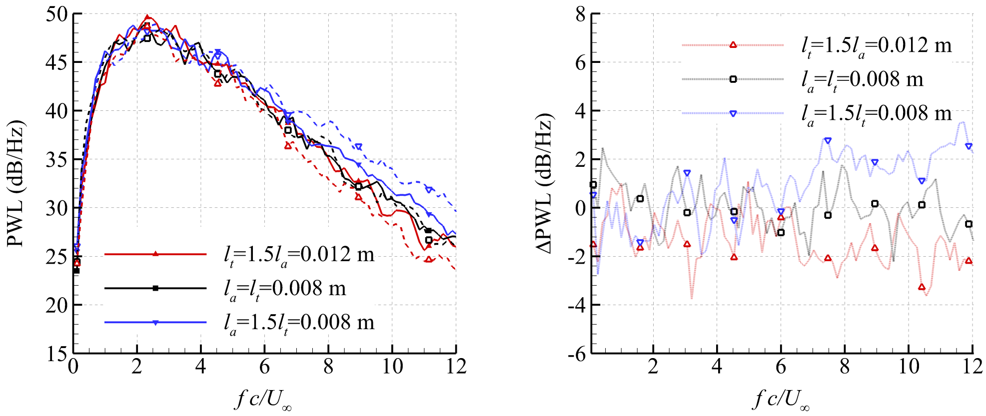

(a) PWL spectra (b) ΔPWL

Figure 6: (a) Noise spectra for a NACA 0012 aerofoil at AoA $= 0°$ *(indicated by the solid lines with solid symbols) and AoA* $= 4°$ *(denoted by the dashed lines with hollow symbols) in anisotropic turbulence with different stretching ratios when* $M_\infty = 0.3$*; (b)* $\Delta\mathrm{PWL} = \mathrm{PWL}|_{AoA=4°} - \mathrm{PWL}|_{AoA=0°}$ *denoted by the dotted lines with hollow symbols.*

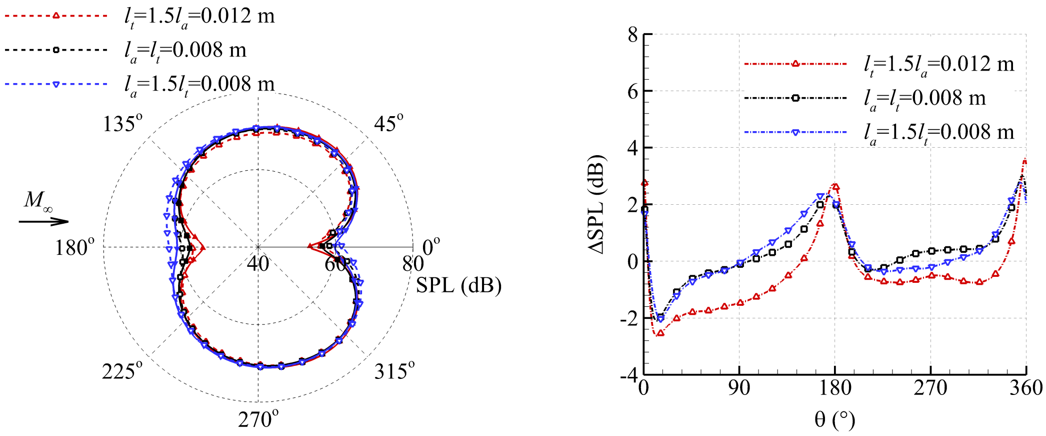

(a) OASPL (b) ΔOASPL

Figure 7: (a) Noise directivity for a NACA 0012 aerofoil at AoA $= 0°$ *(indicated by the solid lines with solid symbols) and AoA* $= 4°$ *(denoted by the dashed lines with hollow symbols) in anisotropic turbulence with different stretching ratios when* $M_\infty = 0.3$*; (b)* $\Delta\mathrm{OASPL} = \mathrm{OASPL}|_{AoA=4°} - \mathrm{OASPL}|_{AoA=0°}$ *denoted by the dash-dotted lines with hollow symbols.*

turbulent eddies are transversely stretched, the noise is reduced at most of the observation angles for the $AoA = 4°$ case, while the most prominent sound reduction also occurs at downstream observers on the suction side of the aerofoil, which is clearly shown in figure 7(b).

4. MODIFIED FAR FIELD NOISE PREDICTION MODEL

In order to improve the far field noise predictions, a modified analytical solution considering the effect of aerofoil thickness is proposed based on the flat plate theory [1]. From what has been discussed above, it can be concluded that it is the distorted transverse energy spectra E_{22} rather than the initial one that plays a significant role in determining the far field noise. Therefore, as shown in Equation 1, the undistorted transverse velocity spectrum $\Phi_{ww}(K_x, 0)$ in the flat plate theory is replaced by the distorted turbulence statistics $\Phi_{ww}^{dis}(K_x, 0)$ sampled at appropriate position.

$$S_{pp}(x, 0, z, \omega) \rightarrow \left(\frac{\omega z \rho_0 b}{c_0 \sigma^2}\right)^2 \pi U d \left|\ell(x, K_x, 0)\right|^2 \Phi_{ww}^{dis}(K_x, 0). \tag{1}$$

The modified analytical solution is compared with the numerical results obtained by RES technique which has been validated against the experiments [13]. Figure 8(a) shows the modified analytical solution of the far field noise directivity for a NACA 0012 aerofoil interacting with isotropic turbulence. The acoustic observation points are $100c$ away from the mid-chord of the aerofoil. Compared with the flat plate theory, the OASPL for the thick aerofoil increases at upstream observers and decreases at downstream observers. Taking the numerical results obtained by RES technique as the baseline, we can see that the modified analytical solution denoted by the black line partly predict the upstream noise increase. While for the downstream observers, some improvements on predicting the downstream noise reduction can also be detected even though they are very small. The validity of the modified far field noise prediction model is evaluated by the SPL derivation from the numerical result, which is defined as the difference between the analytical solution and the numerical result. According to figure 8(b), the modified solution is much closer to the numerical result.

The veracity of the modified analytical solution of anisotropic cases is also verified. As can be seen from figure 9, when the turbulent eddies are stretched in the axial direction, the OASPL around the overhead region is accurately predicted by the modified solution, covering a large range from 70° to 90°. It also shows great improvement for the upstream observation angles, while it cannot capture the downstream noise reduction. Figure 10 shows the performance of the modified far field noise prediction model in the anisotropic case with transverse stretching. For the downstream observers, the modified analytical solution shows improvement in capturing the noise reduction. However, it cannot capture the upstream noise increase, which presents similar deviation from the numerical result compared with the flat plate theory.

Overall, the modified analytical solution prevails over the flat plate theory for all the cases, especially for the axial stretching case and isotropic case. The modified far field noise prediction model partly predicts the upstream noise increase and shows improvement on predicting the downstream noise reduction, based on the accurate description of the distortion around the aerofoil leading edge.

5. CONCLUSIONS

The distortion of anisotropic turbulence spectrum around aerofoil leading edge is investigated in this work. Through the use of RES technique, the anisotropic turbulence with different stretching ratios is synthesized, presenting different levels of distortion

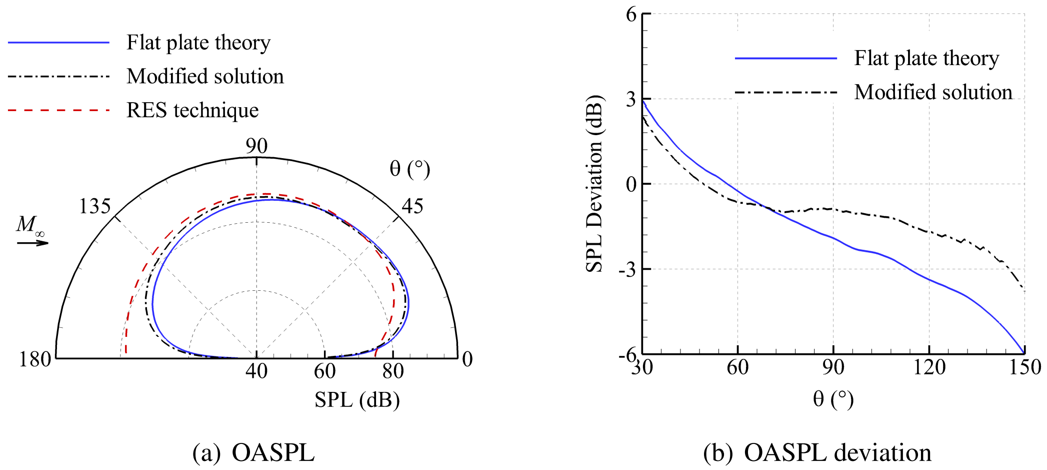

Figure 8: (a) Modified analytical solution of the far field noise directivity for a NACA 0012 aerofoil in isotropic turbulence with $M_\infty = 0.6$; (b) SPL deviation.

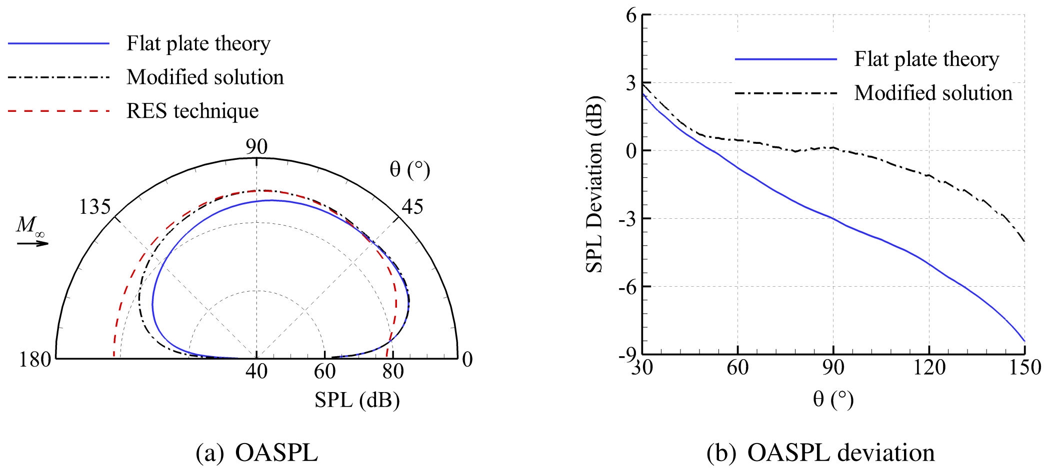

Figure 9: (a) Modified analytical solution of the far field noise directivity for a NACA 0012 aerofoil in axially stretched anisotropic turbulence with $M_\infty = 0.6$; (b) SPL deviation.

depending on the degree of anisotropy in the incident turbulence spectrum. The major findings for the zero incidence cases are as follows:

– For the isotropic case, with the decrease of distance to the stagnation point, the streamwise energy spectra E_{11} show almost uniform reduction at all frequencies compared with the undistorted spectra, whereas the streamwise energy spectra E_{22} increase at low-frequency range and then decrease at high frequencies around the aerofoil leading edge.

– Considering the effect of anisotropy, distortion of the axial stretching case is the smallest, which is reflected in the slightest reduction of energy spectra at high-frequency range. On the contrary, the transverse stretching case shows the most remarkable decrease at high wavenumbers.

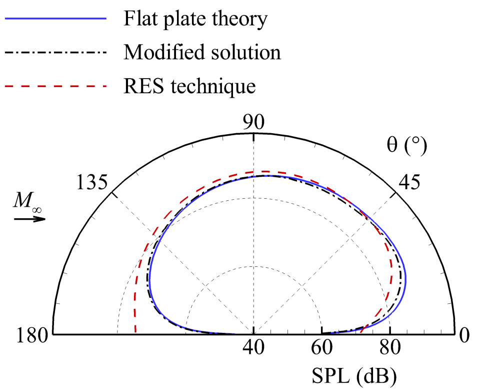

(a) OASPL

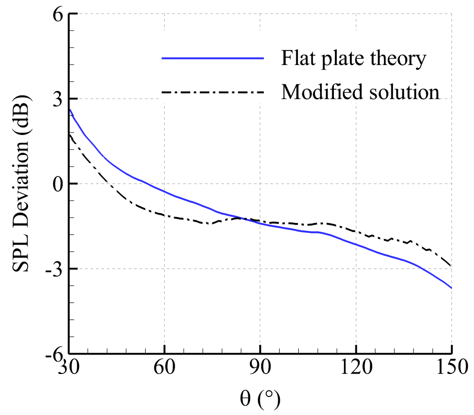

(b) OASPL deviation

Figure 10: (a) Modified analytical solution of the far field noise directivity for a NACA 0012 aerofoil in transversly stretched anisotropic turbulence with $M_\infty = 0.6$; (b) SPL deviation.

In addition, the impact of angle of attack on turbulence distortion and interaction noise is also studied with various incident turbulence spectra characterised by different stretching ratios. It can be concluded that the increase of angle of attack will lead to the increase in the PWL spectra when the eddies are stretched in the axial direction. However, for the anisotropic turbulence with transverse stretching, the increase of incidence will reduce the PWL spectra especially at high frequencies.

Finally, based on Amiet's flat plate theory, a modified analytical solution of the far field interaction noise is proposed, where the distorted turbulence spectra are introduced to account for the effect of aerofoil thickness. The modified noise prediction model shows improvements on predicting the far field noise for thick aerofoils, based on the accurate capture of the distorted anisotropic turbulence spectra in the vicinity of aerofoil leading edge.

6. ACKNOWLEDGEMENTS

Part of the study is supported by Hong Kong Research Grants Council (RGC) Project No.16204316 and No.16203817. Part of the study is supported by National Science Foundation of China (NSFC.11772282). Zhen Shen also wishes to thank Hong Kong University of Science and Technology (HKUST) for supporting part of Ph.D. thesis research. This work was performed in Aerodynamics, Acoustics & Noise Control Technology Centre at HKUST Shenzhen Research Institute (SRI), China (aantc.ust.hk).

7. REFERENCES

[1] R. K. Amiet. Acoustic radiation from an airfoil in a turbulent stream. *Journal of Sound and Vibration*, 41(4):407–420, 1975.

[2] James Gill. *Broadband Noise Generation of a Contra-Rotating Open Rotor Blade*. PhD thesis, 2015.

[3] William R. Sears. Some Aspects of Non-Stationary Airfoil Theory and Its Practical Application. *Journal of the Aeronautical Sciences*, 8(3):104–108, 1941.

[4] J. Gill, X. Zhang, and P. Joseph. Single velocity-component modeling of leading edge turbulence interaction noise. *The Journal of the Acoustical Society of America*, 137(6):3209–3220, 2015.

[5] G. Guidati and S. Wagner. The Influence of Airfoil Shape on Gust-Airfoil Interaction Noise In Compressible Flows. *AIAA Journal*, 279(99-1843):279–286, 1999.

[6] Patrick J Moriarty, Gianfranco Guidati, and Paul Migliore. Recent improvement of a semi-empirical aeroacoustic prediction code for wind turbines. *Proc., 10th AIAA/CEAS Aeroacoustics Conference, Manchester, UK, AIAA*, pages 1–16, 2004.

[7] J Gershfeld. Leading edge noise from thick foils in turbulent flows. *Journal of the Acoustical Society of America*, 116(3):1416–1426, 2004.

[8] Stephane Moreau and Michel Roger. Effect of Angle of Attack and Airfoil Shape on Turbulence-Interaction Noise. In *11th AIAA/CEAS Aeroacoustics Conference*, 2005.

[9] J. C.R. Hunt. A theory of turbulent flow round two-dimensional bluff bodies. *Journal of Fluid Mechanics*, 61(4):625–706, 1973.

[10] Leandro D. Santana, Julien Christophe, Christophe Schram, and Wim Desmet. A Rapid Distortion Theory modified turbulence spectra for semi-analytical airfoil noise prediction. *Journal of Sound and Vibration*, 383:349–363, 2016.

[11] S. A L Glegg and William J. Devenport. Panel methods for airfoils in turbulent flow. *Journal of Sound and Vibration*, 329(18):3709–3720, 2010.

[12] William J. Devenport, Joshua K. Staubs, and Stewart A.L. Glegg. Sound radiation from real airfoils in turbulence. *Journal of Sound and Vibration*, 329(17):3470–3483, 2010.

[13] Zhen Shen and Xin Zhang. Random-eddy-superposition technique for leading edge noise predictions. *2018 AIAA/CEAS Aeroacoustics Conference*, pages 1–14, 2018.

[14] E. J. Kerschen and P. R. Gliebet. Noise Caused by the Interaction of a Rotor with Anisotropic Turbulence. *AIAA Journal*, 19(6):717–723, 1981.

[15] G.I. Taylor. The spectrum of turbulence. *Proceedings of the Royal Society A: Mathematical, Physical and Engineering Sciences*, 164(919):476–490, 1938.

[16] Fernando Gea-Aguilera, Xin Zhang, Xiaoxian Chen, James Gill, and Thomas Nodé-Langlois. Synthetic Turbulence Methods for Leading Edge Noise Predictions. In *21st AIAA/CEAS Aeroacoustics Conference*, number AIAA 2015-2670, 2015.